Phosphatase, $Mg2^{+}/Mn2^{+}$ dependent 1B regulates the hematopoietic stem cell homeostasis via the Wnt/β-catenin signaling

Zhiyuan Lu,[1,2,3*] Hanzhi Yu,[4*] Yanxia Li,[1,2] Guangsen Xu,[1,2] Xiaoxun Li,[1,2] Yongjun Liu,[1,2] Yuemao Shen,[1,2] Zhigang Cai[4] and Baobing Zhao[1,2,5]

[1]Key Laboratory of Chemical Biology (Ministry of Education), School of Pharmaceutical Sciences, Cheeloo College of Medicine, Shandong University, Jinan; [2]NMPA Key Laboratory for Technology Research and Evaluation of Drug Products, School of Pharmaceutical Sciences, Cheeloo College of Medicine, Shandong University, Jinan; [3]School of Pharmaceutical Sciences & Institute of Materia Medica, Shandong First Medical University & Shandong Academy of Medical Sciences, Jinan; [4]The Province and Ministry Co-Sponsored Collaborative Innovation Center for Medical Epigenetics, Department of Pharmacology, School of Basic Medical Science, Tianjin Medical University, Tianjin and [5]Department of Pharmacology, School of Pharmaceutical Sciences, Cheeloo College of Medicine, Shandong University, Jinan, China

**ZL and HY contributed equally as first authors.*

Correspondence: Baobing Zhao
baobingzh@sdu.edu.cn

Received: September 18, 2023.
Accepted: January 31, 2024.
Early view: February 8, 2024.

https://doi.org/10.3324/haematol.2023.284305

©2024 Ferrata Storti Foundation
Published under a CC BY-NC license

Abstract

Hematopoietic stem cells (HSC) are primarily dormant in a cell-cycle quiescence state to preserve their self-renewal capacity and long-term maintenance. How HSC maintain the balance between activation and quiescence remains largely unknown. Herein, we found that phosphatase, Mg^{2+}/Mn^{2+} dependent 1B (Ppm1b) is required for the expansion of phenotypic HSC *in vitro*. By using a conditional knockout mouse model in which *Ppm1b* was specifically depleted in hematopoietic cells, we demonstrated that loss of Ppm1b impaired the HSC homeostasis and hematopoietic reconstitution. Ppm1b deficiency mice also exhibited B-cell leukocytopenia, which is due to the compromised commitment and proliferation of B-biased lymphoid progenitor cells from common lymphoid progenitors. With the aid of a small molecular inhibitor, we confirmed the roles of Ppm1b in adult hematopoiesis that phenocopied the effects with loss of Ppm1b. Furthermore, transcriptome profiling of Ppm1b-deficient HSC revealed the disruptive quiescence of HSC. Mechanistically, Ppm1b interacted with β-catenin and mediated its dephosphorylation. Loss of Ppm1b led to the decrease in the active β-catenin (non-phosphorylated) that interrupted the Wnt/β-catenin signaling in HSC, which consequently suppressed HSC expansion. Together, our study identified an indispensable role for *Ppm1b* in regulating HSC homeostasis via the Wnt/β-catenin pathway.

Supplemental Information

Phosphatase, Mg^{2+}/Mn^{2+} Dependent 1B regulates the self-renewal of HSCs via the Wnt/β-catenin signaling

Zhiyuan Lu[1,2,3#], Hanzhi Yu[4#], Yanxia Li[1,2], Guangsen Xu[1.2], Xiaoxun Li[1,2], Yongjun Liu[1,2], Yuemao Shen[1,2], Zhigang Cai[4], Baobing Zhao[1,2,5*]

[1]Key Laboratory of Chemical Biology (Ministry of Education), School of Pharmaceutical Sciences, Cheeloo College of Medicine, Shandong University, Jinan, China, 250012;

[2]NMPA Key Laboratory for Technology Research and Evaluation of Drug Products, School of Pharmaceutical Sciences, Cheeloo College of Medicine, Shandong University, Jinan, Shandong 250012, China

[3]School of Pharmaceutical Sciences & Institute of Materia Medica, Shandong First Medical University & Shandong Academy of Medical Sciences, Jinan, China, 250117;

[4]The Province and Ministry Co-Sponsored Collaborative Innovation Center for Medical Epigenetics, Department of Pharmacology, School of Basic Medical Science, Tianjin Medical University, Tianjin, China, 300070;

[5]Department of Pharmacology, School of Pharmaceutical Sciences, Cheeloo College of Medicine, Shandong University, Jinan, China, 250012;

#These authors contributed equally to this work.

*Correspondence to:
Baobing Zhao, Ph.D., Department of Pharmacology, School of Pharmaceutical Sciences, Shandong University, 44 W Wenhua Road, Jinan, Shandong, P.R.China, 250012; baobingzh@sdu.edu.cn; TEL/FAX: +86-531-88382176.

Supplementary Files:

Supplementary Methods

Generation of *Ppm1b* conditional knockout mice mice

The Ppm1b conditional knockout mice were created via CRISPR/Cas9-mediated genome engineering. In brief, donor, sgRNA, and Cas9 mRNA were co-injected into zygotes. Cas9 endonuclease was guided to cleave introns 1-2 and 2-3 by the sgRNAs (5'- AGTATGGTTGAACTGCG-3' and 5'-GCGGCAGTTAGAATTA-3'), causing a double-strand break. LoxP sites were inserted into intron 1-2 and intron 2-3 respectively by homologous recombination and verified by DNA sequencing. Standard techniques were used to create chimeric mice. ***Ppm1b*** deletion was achieved by crossing with transgenic Vav-cre mice purchased from JAX Lab (B6.Cg-Commd10Tg(Vav1-icre)A2Kio/J), by which Exon 2 floxed by loxP sites were deleted in hematopoietic cells. Ppm1b expression was disrupted as a result. Ppm1b $^{fl/fl}$ littermate mice were genotyped by PCR with primers ***Ppm1b***-tF1 (5'-TGTGCCAGTGTAGATGAACCAAC-3') and ***Ppm1b***-tR1(5'-CCACCACAAAGTTATCAAGGCTAG-3'). Excision after Vav-Cre recombination was confirmed by PCR with primers to detect a portion that remains post excision (***Ppm1b***-null-TF1:5'-TGTGCCAGTGTAGATGAACCAAC-3' and ***Ppm1b***-null-TR1: 5'-AGGAAGAATAAAGCAGGAAGCCTG -3').

Homing assay

2×10^6 BMMCs (CD45.2) from Ppm1b^{CKO} or Ppm1b$^{fl/fl}$ mice were injected retro-orbitally into lethally irradiated (8.5 Gy X-ray) WT recipient mice (CD45.1). The BM cells were harvested after 18 h injection and the frequency of donor-derived cells (CD45.2) was analyzed by flow cytometry.

Quantitative real-time PCR

RNA isolation, cDNA synthesis and qRT-PCR were performed as previously described.[1, 2] Briefly, total RNA was using TRIzol™ Reagent (ThermoFisher)

and cDNA was synthesized using PrimeScript RT reagent Kit with gDNA Eraser (Takara), following manufacturer's instructions. Then, qRT-PCR assay was performed by using SYBR Green Master Mix (Takara) on QuantStudio 3 (ThermoFisher). Relative gene expressions were analyzed with the comparative CT (ΔΔCT) method and normalized to 18S rRNA. Detailed primers used in this study are listed in Supplementary Table 4.

Colony-forming assay

2×10^4 BMMCs were cultured in 1ml of methylcellulose medium (Methocult M3630, StemCell) containing human interleukin 7 in six-well plates. After incubation at 37 °C with 5% CO_2 for 7 days, the colonies were scored with an Axio Observer A1 microscope (ZEISS) and the area of colony was evaluated with ImageJ software (NIH).

Cell cycle assay

Cells were stained with indicated surface markers and fixed and permeabilized using Foxp3 Staining Buffer Set (ebioscience). Then, cells were incubated with FITC-Ki67 and Hoechst 33342 (Sigma) for more than 30 min on ice. Cell cycle was analyzed by flow cytometry and Flowjo software.

Flow cytometric assays

Briefly, for peripheral blood (PB) analysis, 20 μL of PB were lysed with red blood cell lysis buffer (ThermoFisher) and washed by centrifugation at 6000 × g for 5 min before the cells were stained with FITC-B220, APC-CD3e, Pacific Blue-Gr-1, PE-CD11b, PE-Cy7-CD45.2 and Brilliant Violet 605-CD45.1 in FACS buffer. Lineage-negative cells were isolated from bone marrow compartments using a Mouse Hematopoietic Progenitor Cell Enrichment Set (BD Pharmingen), and were then incubated with FITC-Sca1 (Ly-6A/E), APC-CD117 (c-Kit), PE/cy7-CD34, PE-CD135, and Pacific Blue-CD16/CD32 for characterization of different cell populations. For analyses of SLAM-LSK, lineage-negative cells were stained with FITC-Sca1(Ly-6A/E), APC- CD117(c-Kit), APC/cy7-CD48 and PE-

CD150. For analyses of CLPs, the cells were stained with FITC-Sca1 (Ly-6A/E), APC- CD117 (c-Kit) and PE-CD127 (IL-7Ra). For B cell development analysis, the cells were stained with FITC-B220, APC- IgM, PE-IgD, Pacific Blue-CD24 and PE/cy7-CD43. The detailed information for antibodies were provided in Supplementary Table 3.

Bulk Transcriptomic Analysis

Raw sequencing data were processed employing the TrimGalore toolkit to cleanse low-quality reads and eliminate Illumina sequencing adapters. Subsequently, FastQC [3] was utilized for quality control of the processed data. Reads were mapped to mouse reference genome files using the Hisat2 alignment tool. FeatureCounts efficiently computed the number of reads attributed to genomic features (exons), generating the original count matrix for subsequent analyses. The R package "edgeR" [4] processed raw counts and employed a paired design to identify DEGs between the two mouse LSK populations. DEGs exhibiting |logFC| > 0.5 and p-values < 0.05 were deemed statistically significant and employed for Gene GO and Kyoto Encyclopedia of Genes and Genomes (KEGG) analyses.

Single-Cell RNA Sequencing

Hematopoietic stem cells derived from $Ppm1b^{CKO}$ mice and $Ppm1b^{fl/fl}$ mice were incorporated into a Chromium™ Single Cell Gene Expression System (10XGenomics) to produce gel beads in emulsions (GEMs), consisting of gel beads (containing pre-fabricated 10x primers), individual cells, and Master Mix. Within the GEMs, cell lysis and reverse transcription reactions were executed, facilitating the ligation of 10x Barcodes to the complementary DNA (cDNA) products. Following this, the GEMs were disrupted, and polymerase chain reaction (PCR) amplification was carried out, employing cDNA as the template. Post amplification, libraries were assembled in accordance with the 10×Genomics 3' gene expression protocol, and sequencing was performed

utilizing the Illumina NovaSeq sequencing platform. Subsequently, raw data from each sample were processed via cellranger (version 3.1.0) [29], aligning the reads to the mouse genome (mm10) and generating a gene-cell matrix for subsequent analyses.

Single-Cell Transcriptomic Analysis

Raw feature-barcode matrices were imported into the Seurat package (version 4.3.0) [30] for downstream analyses. To eliminate low-quality cells and multiple captures, cells exhibiting >6500 or <2000 expressed genes, >20% unique molecular identifiers (UMIs) linked to the mitochondrial genome, or >40% UMIs associated with the ribosomal genome were excluded from further analysis using the subset function. Data normalization and standardization were achieved through the utilization of sctransform in Seurat, mitigating the impact of technical factors such as sequencing depth. Dimensionality reduction was performed employing the principal component analysis (PCA) algorithm, identifying significant principal components (50 PCs) for subsequent clustering via the ElbowPlot function. The FindClusters function were employed with a relatively high resolution (2.2) to ensure precise clustering and annotation of HSCs. Visualization of single-cell data was accomplished through the nonlinear dimensionality reduction algorithm UMAP. The FindAllMarkers function within the Seurat package was used to identify cluster-specific marker genes, and significant gene signatures (p_val_adj < 0.001) were examined using the R clusterProfiler package [31] for Gene Ontology (GO) category enrichment. Genetic markers from myeloid, lymphoid, megakaryocytic, and erythroid lineages were employed to annotate cell populations, while enrichment analysis outcomes were also considered, designating corresponding clusters as pMy, pLy, pMk, and pEr. A subset of hematopoietic stem cells (HSCs) exhibiting no specific lineage differentiation propensity and characterized by self-renewal was denoted as non-primed. The FindMarkers function in Seurat was utilized to compare differentially expressed genes (DEGs) between the $Ppm1b^{CKO}$ and

Ppm1b$^{fl/fl}$ groups within each annotated cell population. GO pathway enrichment analysis of the generated DEGs was subsequently conducted, with $P < 0.05$ considered significantly enriched. RNA sequencing data that support the findings of this study were deposited in NCBI SRA under accession number GSE237748.

Statistical analysis

All statistical analyses were performed with GraphPad Prism 9. All data are presented as mean ± SD. All comparisons were tested using unpaired two-tailed Student's t-test or one-way ANOVA as described in the figure legends. A *P* value of less than 0.05 was considered statistically significant. Blinding was performed for *in vitro* experiments with data analysis by different operators.

Supplementary Figure legends

Figure S1 Ppm1b inhibition led to the repressed proliferation of HSPCs, related to Figure 1.

(**A**) Quantitative PCR analysis of *Ppm1b* levels of in the indicated lineage cells from bone marrow. 18S ribosomal RNA was used as an internal control. Data were presented as mean ± SD from three independent experiments. (**B**) Lineage-negative cells from mouse bone marrow were cultured *in vitro* with the treatment of HN252 (0, 5, 10, and 20 μM) for 48 h. The relative proliferation ratio of LK (Lin$^-$c-Kit$^+$) cells was quantified by flow cytometry, and normalized to the uncultured cells. Data were presented as mean ± SD from three independent experiments. (**C**) Flow cytometric analysis of apoptosis in LSK (Lin$^-$Sca-1$^+$c-Kit$^+$) cells from the cells as in Figure 1B. Representative flow

cytometric profiles of apoptosis were shown on the left. Data were presented as mean ± SD from three independent experiments. *P* values were determined by 1-way ANOVA with Tukey's multiple comparisons test (B) or using unpaired two-tailed Student's t-test (C). ***$P < 0.001$ and ****$P < 0.0001$.

Figure S2 Loss of Ppm1b impaired B cell development, related to Figure 2.

(**A**) Schematic of $Ppm1b^{fl/fl}$ Vav-Cre ($Ppm1b^{CKO}$) mice gene-targeting strategy. (**B**) Quantitative PCR analysis of *Ppm1b* levels in mononuclear cells from bone marrow and peripheral blood of indicated mice. 18S ribosomal RNA was used as an internal control. Data were presented as mean ± SD from three independent experiments. (**C**) The cell counts of neutrophils, monocytes, red blood cells (RBC) and platelets in peripheral blood from indicated mice at the age of 8 weeks. K: $x10^3$; M: $x10^6$. Data were shown as mean ± SD. Each dot represents one mouse. (**D**) Flow cytometric analysis of the ratio of Myeloid, B Cells, and T cells in peripheral blood from (A), n=5. (**E**) Representative flow cytometric profiles of the strategy for gating B cell compartment in bone marrow. $B220^+$ BM cells were subdivided into mature B cells ($B220^+IgM^{+/-}IgD^+$), immature B cells ($B220^+IgM^+IgD^-$), pre-pro B cells ($B220^+IgM^-IgD^-CD43^+CD24^-$), pro B cells ($B220^+IgM^-IgD^-CD43^+CD24^+$), and pre B cells ($B220^+IgM^-IgD^-CD43^-CD24^+$). (**F-I**) Statistical analysis of the percentage of indicated B lymphoblasts in bone marrow from indicated mice, n=4. Data were presented as mean ± SD. (**J**) Quantification of the thymus

weight from indicated mice as in D, n=7. (**K**) Representative flow cytometric profiles of T lymphoblasts in the thymus. (**L**) Statistical analysis of the frequencies of indicated T lymphoblasts as in H, n=4. (**M**) Quantification of the area of colonies in Figure 2 E, n=21-35. Data are presented as mean ± SD from three independent experiments. Data were presented as mean ± SD. All *P* values were determined by unpaired two-tailed Student's t-test.

Figure S3 Loss of Ppm1b decreased the functional HSCs *in vivo*, related to Figure 3.

(**A**) Representative flow cytometric profiles of LSK cells of 8 weeks old $Ppm1b^{CKO}$ and $Ppm1b^{fl/fl}$ mice. (**B**) Statistical analysis of the percentage and number of LK cells from indicated mice as in (A), n=4. (**C**) Representative flow cytometric profiles of the gating strategy of the subset of LSK from $Ppm1b^{CKO}$ and $Ppm1b^{fl/fl}$ mice. (**D**) Statistical analysis of the percentage of SLAM-LSK cells from indicated mice in (B), n=4. (**E**) HSC homing assay: percentage of CD45.2 cells in the BM after 18 hours injection of 2×10^6 BM cells into irradiated CD45.1 mice, n=6. **(F)** Lineage negative cells purified from indicated mice were labelled with CFSE and cultured for 48 h *in vitro*. The fluorescence intensity of CFSE in LSK cells was quantified by flow cytometry, n=3. **(G)** Cell cycles of LSK cells from the indicated mice which were administrated with a single dose of 5-FU for eight days were analyzed, n=4. **(H)** Schematic diagram showing competitive bone marrow transplantation (mixed ratio, 1:1). **(I)** Chimerism studies of peripheral blood mononuclear cells derived from $Ppm1b^{CKO}$ and

Ppm1b$^{fl/fl}$ mice after competitive transplantation at indicated time points, n=6. (**J**) Percentage of donor-derived SLAM-LSK cells in the BM of the primary and secondary recipient mice, n=6. (**K**) Statistical analysis of the peripheral blood B cells derived from Ppm1b^{CKO} and Ppm1b$^{fl/fl}$ mice after competitive transplantation at indicated time points, n=6. (**L**) Percentage of donor-derived B cells in the BM of the primary and secondary recipient mice, n=4. *P < 0.05, **P < 0.01, ***P < 0.001. All P values were determined by unpaired two-tailed Student's t-test. Data are presented as mean ± SD from three independent experiments.

Figure S4 HN252 affect the HSC pool and B cell differentiation in adult hematopoiesis via targeting Ppm1b, related to Figure 4.

(**A**) Quantification of platelets and red blood cells in peripheral blood at indicated time points from the mice in Figure 4A during HN252 injection, n=6. (**B**) The Ppm1b^{CKO} mice were treated with HN252 or not as in Figure 4A, and the white blood cells and lymphocytes in peripheral blood at indicated time points were analyzed during HN252 injection, n=6. (**C-D**) The number of B cells (C) and the percentage of LSK cells (D) from indicated mice in (C) were measured by flow cytometry after a single dose of 5-FU administration for 8 days, n=4. (**E**) Lineage negative cells purified from indicated mice were labeled with CFSE and cultured with HN252 or not for 48 h *in vitro*. The fluorescence intensity of CFSE in LSK cells were quantified by flow cytometry, n=3. *P < 0.05. All P values were determined by unpaired two-tailed Student's t-test. Data are

presented as mean ± SD from three independent experiments.

Figure S5 Ppm1b plays a crucial role in the regulation of B cell development, related to Figure 5.

(**A**) The volcano plot displaying (Differentially expressed genes) DEGs between $Ppm1b^{CKO}$ and $Ppm1b^{fl/fl}$ lineage negative cells, as determined via bulk RNA-seq, with Wnt pathway genes highlighted ($P < 0.05$). (**B**) Gene Set Enrichment Analysis of B cell activation and immunoglobulin production in lineage-negative cells from $Ppm1b^{CKO}$ and $Ppm1b^{fl/fl}$ mice. (**C**) Quantification of the mRNA expression of indicated genes in $B220^{+}$ cells from $Ppm1b^{CKO}$ and $Ppm1b^{fl/fl}$ mice. Transcripts were normalized to 18S ribosomal RNA. (**D**) Quantification of the protein levels of FOXO1 in indicated cells in (C) by flow cytometry. $*P < 0.05$, $**P < 0.01$, $***P < 0.001$, $****P < 0.0001$. All *P* values were determined by unpaired two-tailed Student's t-test. Data are presented as mean ± SD from three independent experiments.

Figure S6 Transcriptome profiling of PPM1B-deficient HSCs reveals altered stem cell properties, related to Figure 5.

(A) A UMAP plot of 7,364 LSK cells, partitioned into 24 clusters via unsupervised clustering (resolution = 2.2). **(B)** Sample origin. Green: $Ppm1b^{fl/fl}$ group. Red: $Ppm1b^{CKO}$ group. **(C)** Bar chart shows the cellular fractions of LSK cells from $Ppm1b^{CKO}$ and $Ppm1b^{fl/fl}$ mice, respectively.

Figure S7 Ppm1b is involved in the regulation of Wnt/β-catenin pathway

***in vivo* and *in vitro*, related to Figure 6.**

(**A**) Representative flow cytometric profiles of the fluorescence intensity of active β-catenin after being treated by HN252 for different hours. (**B**) Quantification of the mean fluorescence intensity of active β-catenin in (B). (**C**) Quantification of the mRNA level of *cyclin D1* and *Myc* in (B). Transcripts were normalized to 18S ribosomal RNA. **(D)** Lineage negative cells purified from $Ppm1b^{CKO}$ mice were cultured with or without BML-284 (10 nM) for 48 h *in vitro*, and the mRNA level of *cyclin D1* and *Myc* were quantified by qPCR. Transcripts were normalized to 18S ribosomal RNA. **(E)** Lineage negative cells purified from indicated mice were labelled with CFSE, and then the cells were cultured with or without BML-284 (10 nM) for 48 h *in vitro*. The number of LSK cells was quantified by flow cytometry. (**F**) The $Ppm1b^{CKO}$ and $Ppm1b^{fl/fl}$ mice were treated with BML-284 (5 mg/kg) or not for 4 days, and followed by a single dose injection of 5-FU for another 7 days. The number of LSK cells was determined from indicated mice by flow cytometry, n=4. $^{**}P < 0.01$. All *P* values were determined by unpaired two-tailed Student's t-test. Data are presented as mean ± SD from three independent experiments.

Supplementary Fig.1

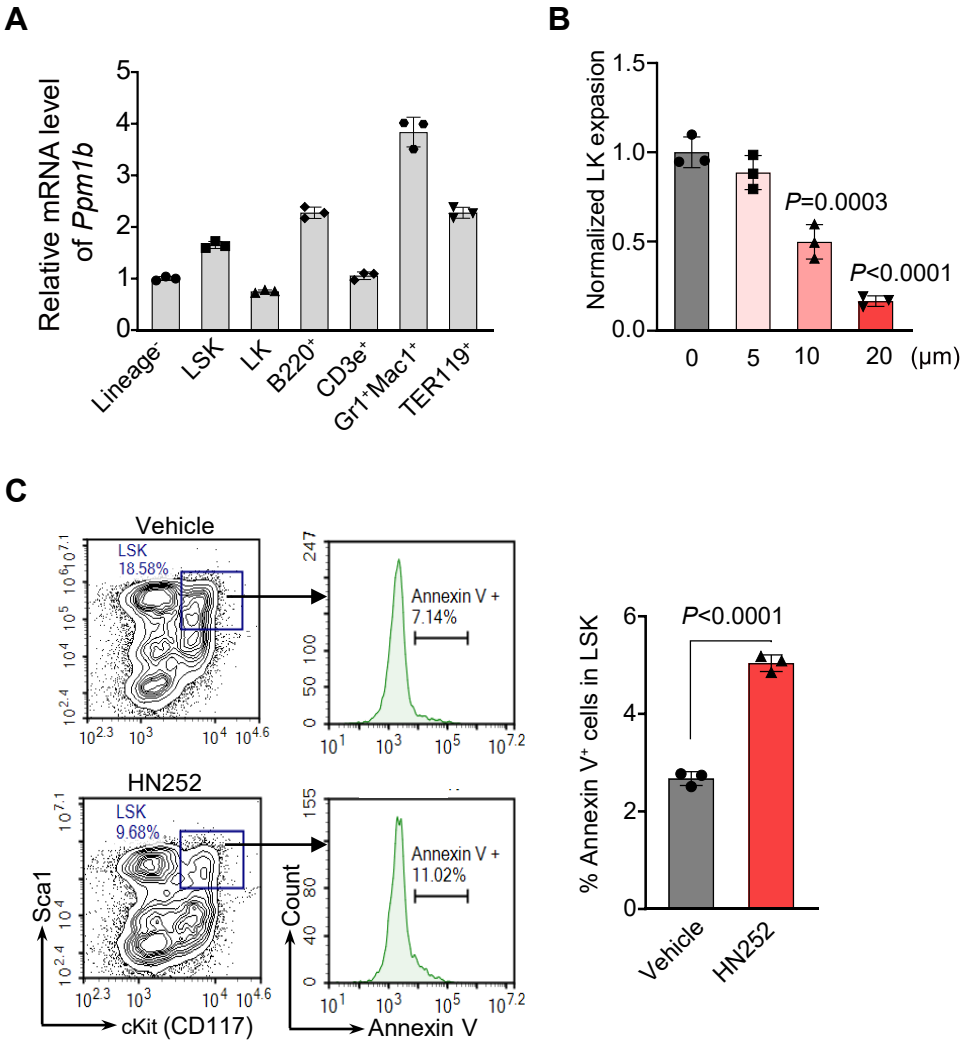

Supplementary Fig.2

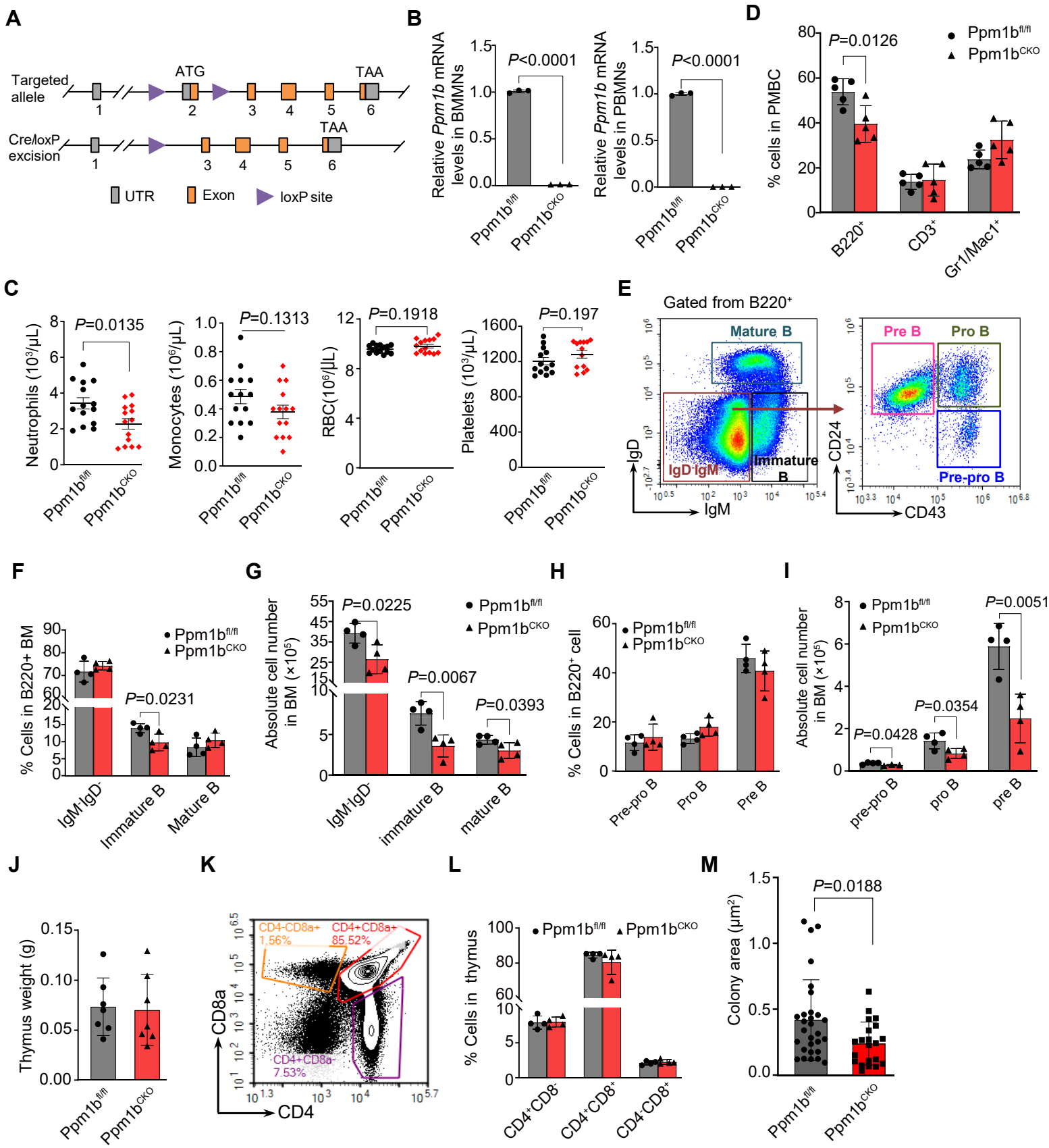

Supplementary Fig.3

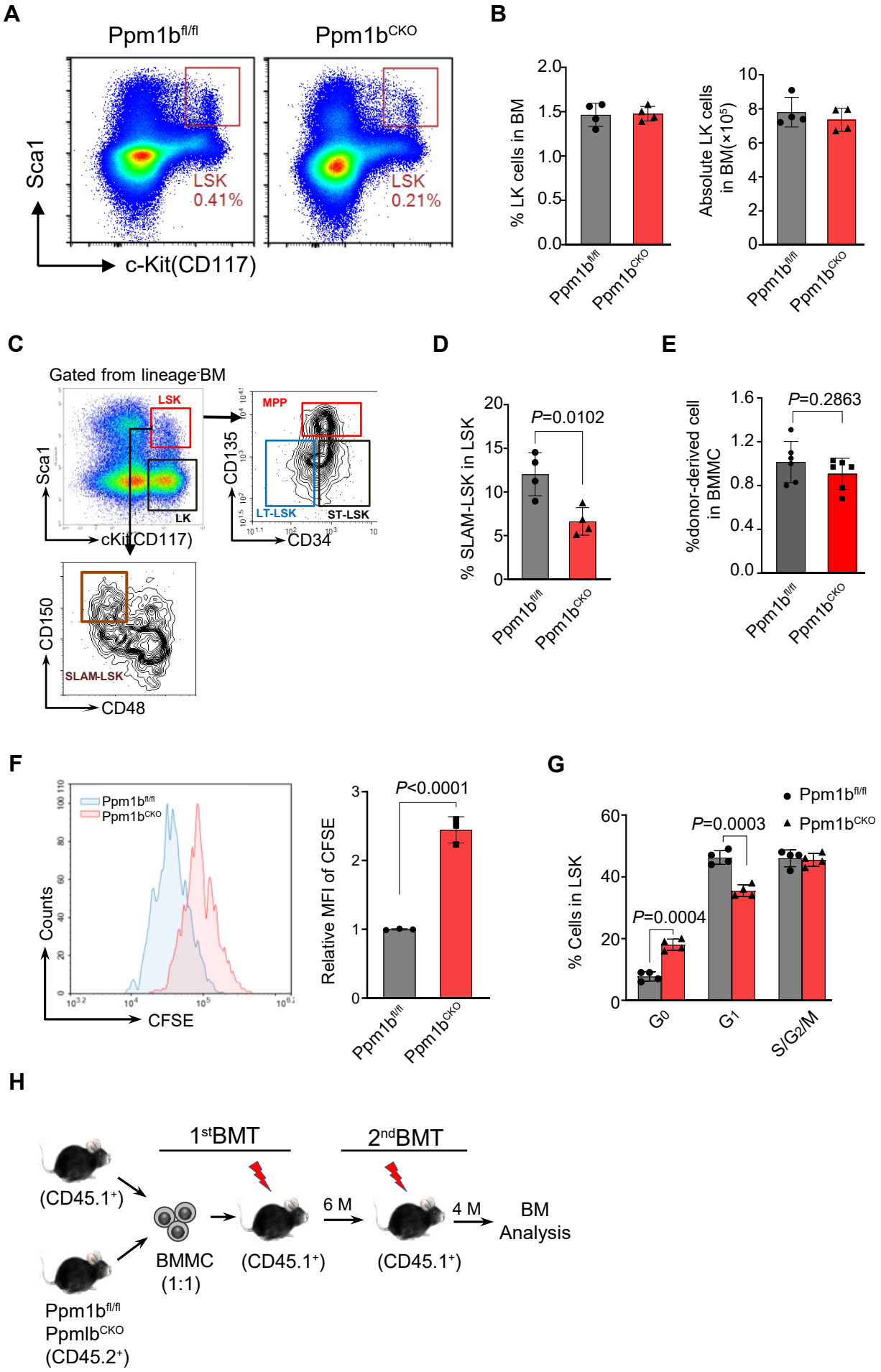

I

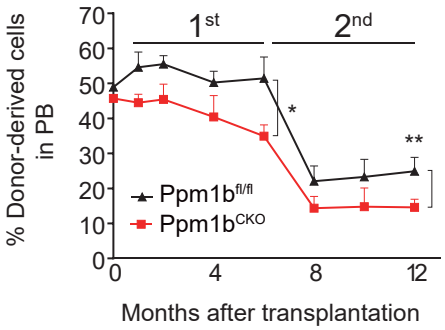
% Donor-derived cells in PB
1st
2nd
*
**
Ppm1bfl/fl
Ppm1bCKO
Months after transplantation

J

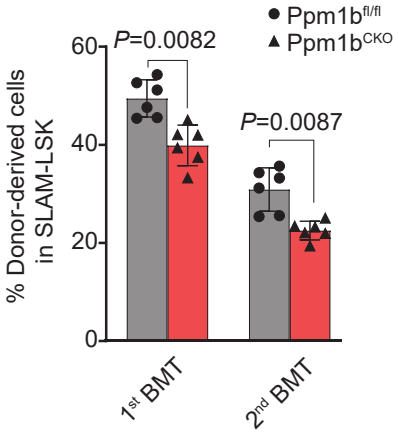
Ppm1bfl/fl
Ppm1bCKO
P=0.0082
P=0.0087
% Donor-derived cells in SLAM-LSK
1st BMT
2nd BMT

K

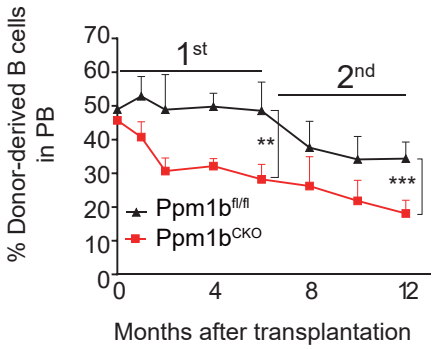
% Donor-derived B cells in PB
1st
2nd
**
***
Ppm1bfl/fl
Ppm1bCKO
Months after transplantation

L

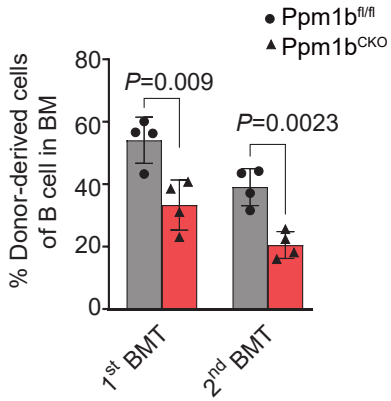
Ppm1bfl/fl
Ppm1bCKO
P=0.009
P=0.0023
% Donor-derived cells of B cell in BM
1st BMT
2nd BMT

Supplementary Fig.4

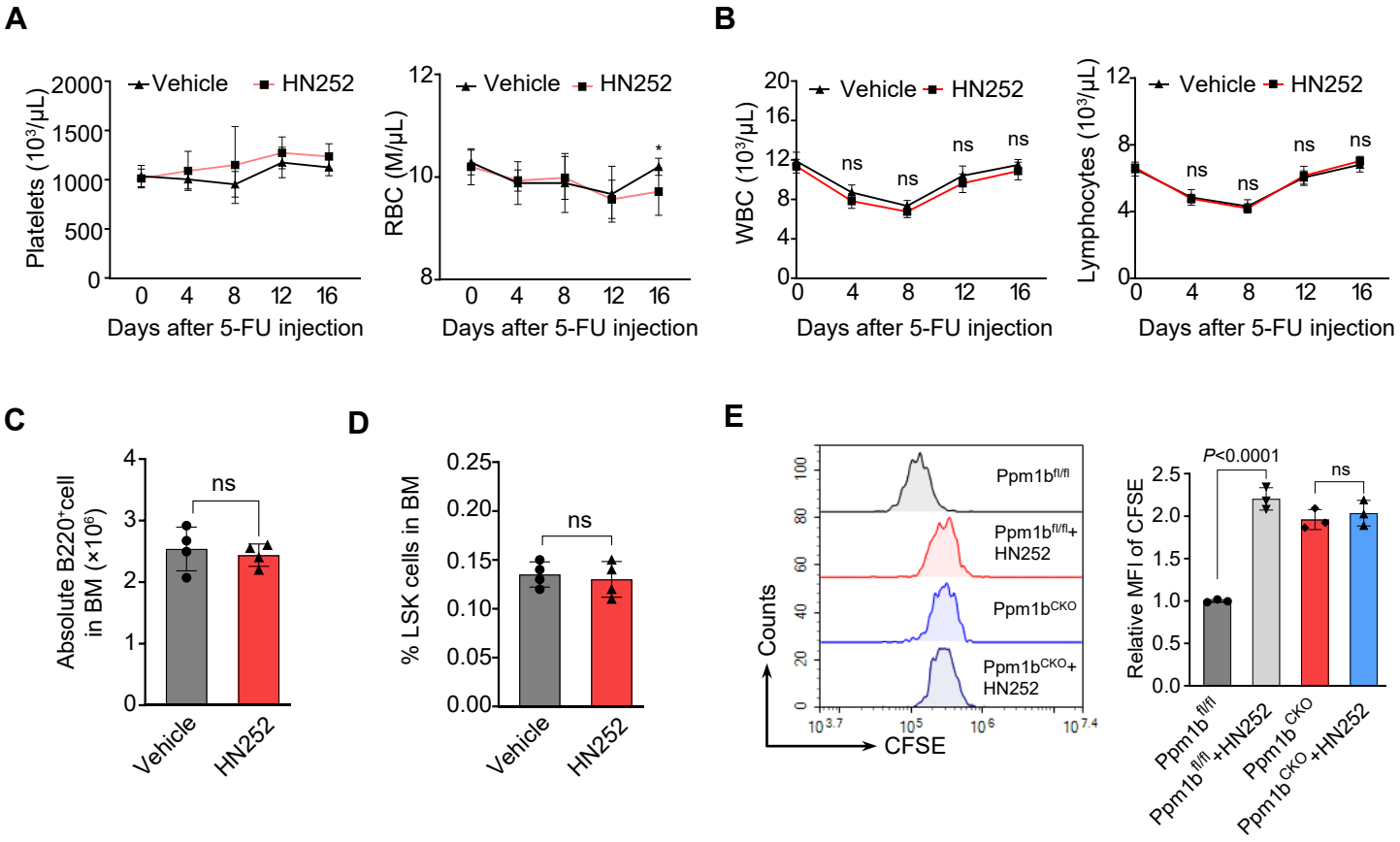

Supplementary Fig.5

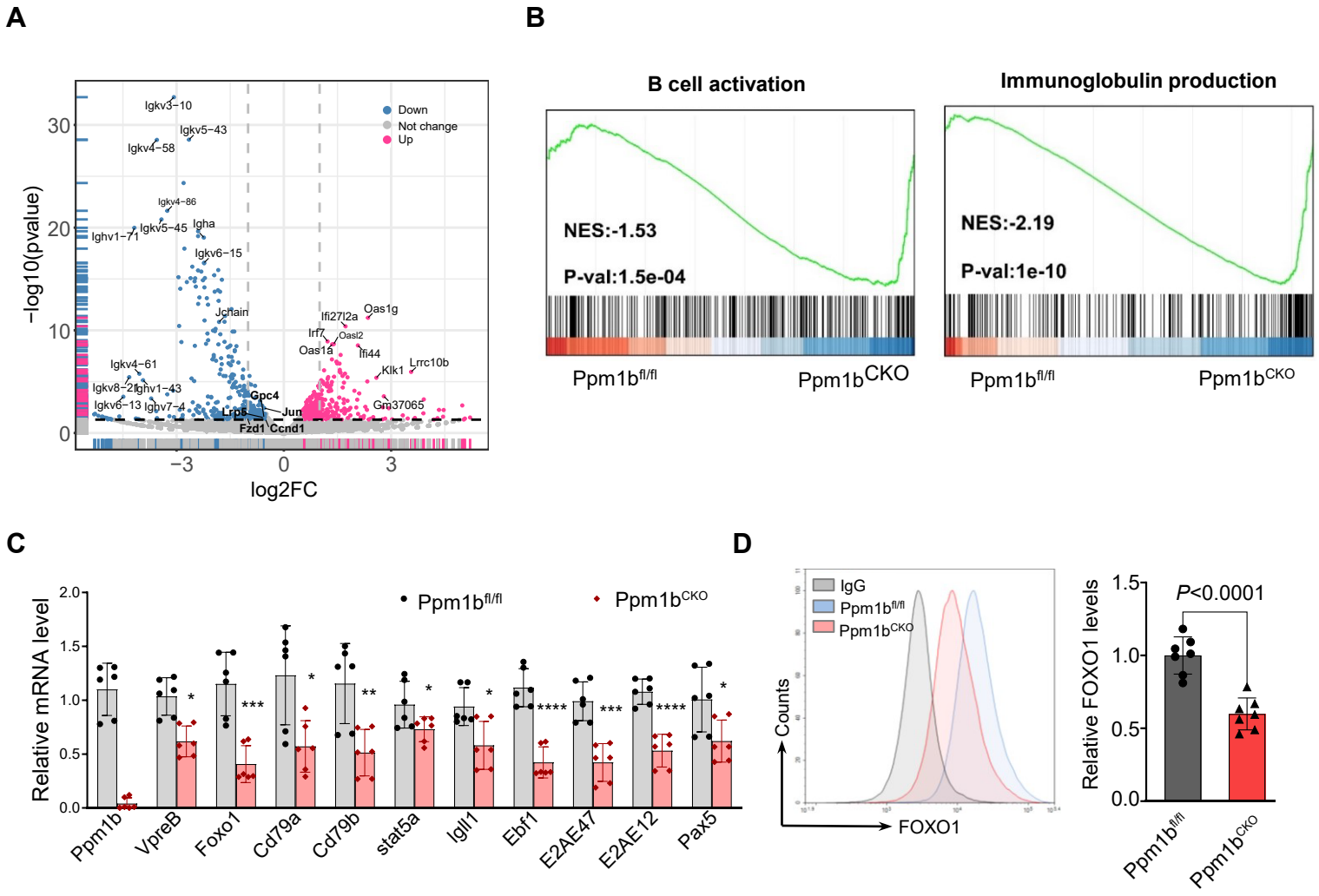

Supplementary Fig.6

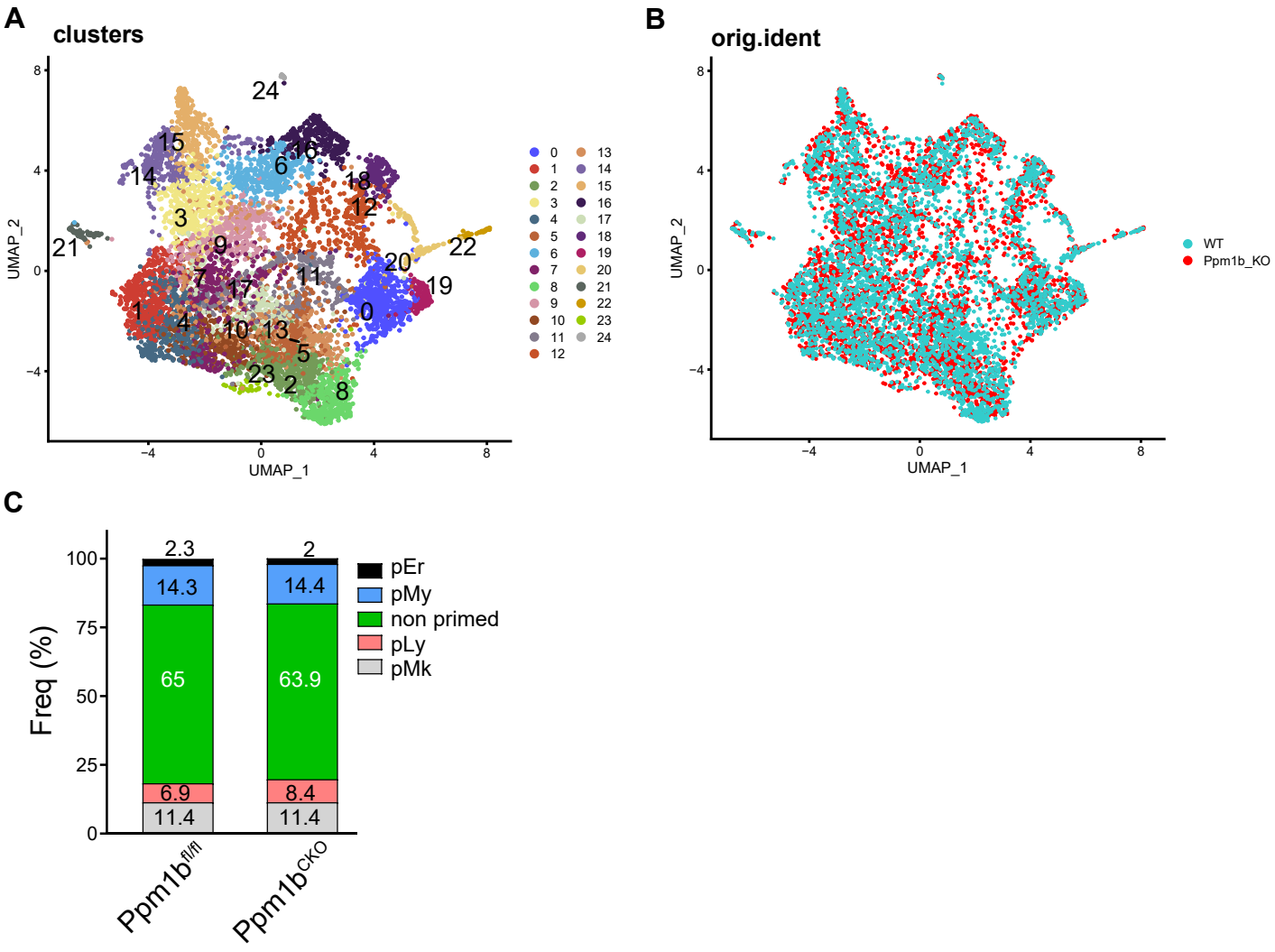

Supplementary Fig.7

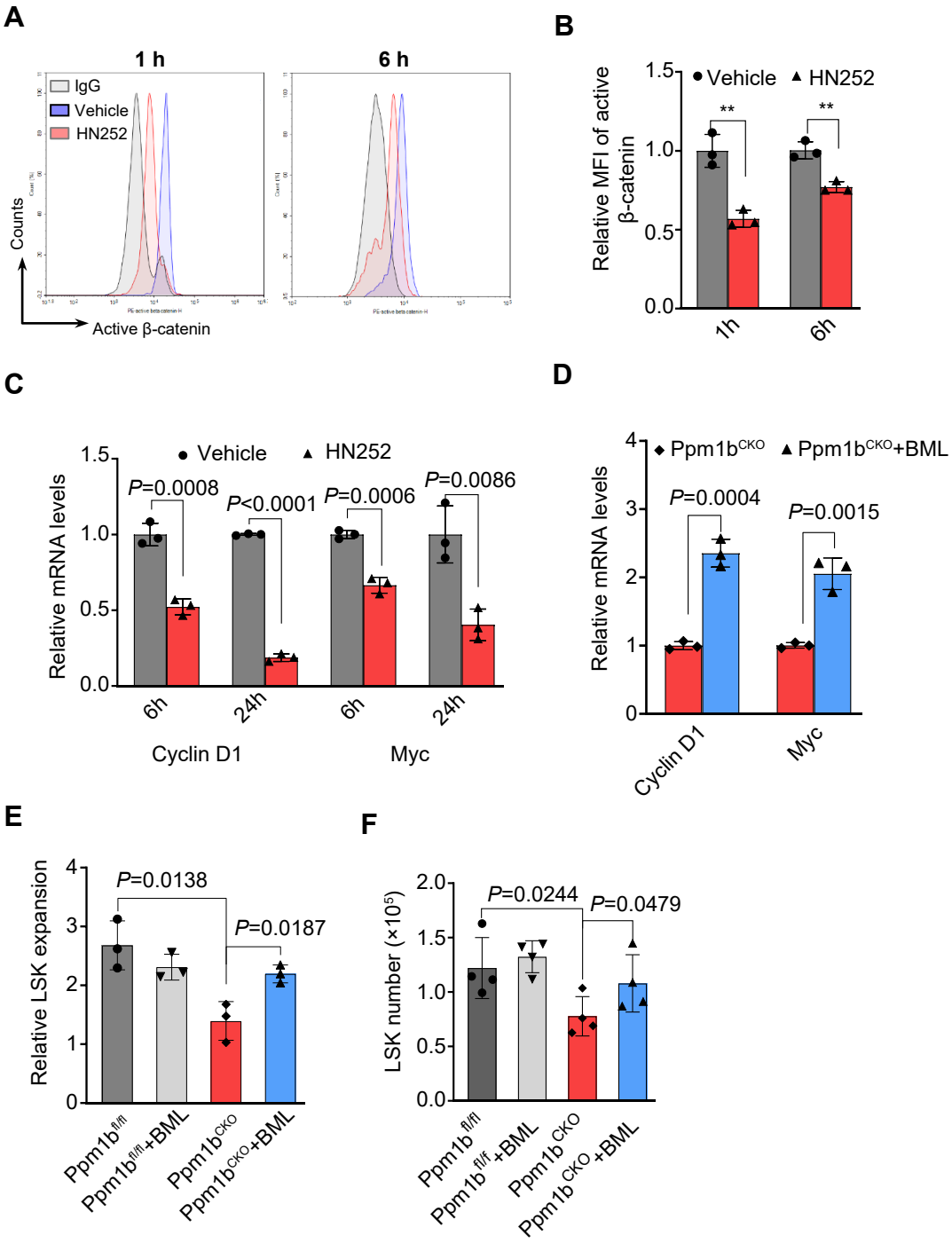

Supplementary Tables (see excel files)

Table S1 Gene Set Enrichment Analysis of genes upregulated and downregulated in Ppm1b^{CKO} group (*p* value< 0.01; FDR *q* value <0.01).

Table S2 Gene differential expression analysis in the non-primed cluster in Ppm1b^{CKO} group (*p* value< 0.01; FDR *q* value <0.01).

Table S3. Antibodies and commercial reagents were used in this study.

Table S4. Primer sequences were used in this study.

References

1. Zhao B, Mei Y, Cao L, et al. Loss of pleckstrin-2 reverts lethality and vascular occlusions in JAK2V617F-positive myeloproliferative neoplasms. J Clin Invest. 2018;128(1):125-140.

2. Mei Y, Han X, Liu YJ, Yang J, Sumagin R, Ji P. Diaphanous-related formin mDia2 regulates beta2 integrins to control hematopoietic stem and progenitor cell engraftment. Nat Commun. 2020;11(1):3172.

3. de Sena Brandine G, Smith AD. Falco: high-speed FastQC emulation for quality control of sequencing data. F1000Res. 2019; 8:1874.

4. Robinson MD, McCarthy DJ, Smyth GK. edgeR: a Bioconductor package for differential expression analysis of digital gene expression data. Bioinformatics. 2010;26(1):139-140.